Original Article :

Structural studies on azadirachtin targeting the glucuronosy ltransferase from lymphatic filariasis and its inhibition.

Esam S. Al-Malki

Department of Biology, College of Science, Majmaah University, Al-Majmaah 11952, Saudi Arabia

Received on Dec 02, 2023, accepted for publication on Jan 20, 2024, dx.doi.org/10.5455/mjhs.2024.02.008

Corresponding author:
Esam S. Al-Malki
Department of Biology, College of Science, Majmaah University, Al-Majmaah 11952, Saudi Arabia,
E.mail: e.almalki@mu.edu.sa, Telephone : + 966504111165

OPEN ACCESS Distributed under Creative Commons CC BY-NC-ND 4.0

Abstract

Background and Aims:
Brugia malayi, Brugia timori, and Wuchereria bancrofti are parasitic worms that cause lymphatic filariasis, also known as elephantiasis in some parts of the world. Because no effective vaccines and current treatments have adverse pharmacological properties, this condition has sparked much interest in the drug discovery community. This research aims to assess the efficacy of azadirachtin against a possible therapeutic target, intestine glucuronosyltransferase protein, in treating and preventing lymphatic filariasis.

Methods:
I-Tasser was used to create the protein, Uniprot was used to collect its FASTA sequences, and Galaxy Refine was used to refine the protein model. The protein 3D model was tested using PROCHECK and ERRAT. We used PubChem to get the three-dimensional structure of the azadirachtin ligand molecules. To study the toxicity profiles and pharmacokinetics, researchers employ SwissADME. Molecular docking studies were conducted using the AutoDock tool, and Pymol viewer was used to observe the interactions between the target protein and the ligand molecules.

Results:
The azadirachtin compound has a satisfactory range of pharmacokinetic parameters in terms of its absorption, distribution, metabolism, and excretion. When compared to the currently existing drug Diethylcarbamazine, molecular docking studies indicate that the azadirachtin molecule binds with the intestinal glucuronosyltransferase proteins of Brugia timori, Wuchereria bancrofti, and Brugia malayi strongly.

Conclusions:
In sum, our understanding of the mechanism by which azadirachtin, a traditional component derived from plants, inhibits intestinal glucuronosyltransferase protein is enhanced, and this could pave the way for the development of new targeted anti-filarial agents.

Keywords:
Filariasis, azadirachtin, Diethylcarbamazine, Anti- microfilarial activity, molecular docking, Molecular modelling, ADMET prediction.

Introduction

Lymphatic filariasis, commonly known as elephantiasis, is a parasitic infection caused by the filarial nematodes Brugia malayi(BM), Wuchereria bancrofti(WB) and Brugia timori(BT). W. bancrofti is prevalent in the Philippines, Papua New Guinea, South East Asia, and tropical Africa [1]. Comparing W. bancrofti to other Lymphatic filarial worms, the latter typically have a body length ranging from 309.2 µm to 346.8 µm. B. malayi is found in South and Southeast Asia, coexisting in some areas with W. bancrofti. B. malayi often have smaller bodies, measuring between 205 and 240 µm in length[2]. The distribution of B. timori is limited to the smaller Indonesian Sunda Islands, and the only known vector of this parasite is Anopheles barbirostris. These parasites are transmitted to humans through several mosquito species, particularly Anopheles, culex, Aedes, and Mansonia. Mosquitoes can spread lymphatic filariasis from infected humans by ingesting microfilariae, tiny worms circulating in contaminated blood[3]. After that, the little worms travel to the human lymph veins through the infected mosquito bite wounds. As they mature in the lymph vessels, they obstruct the lymphatic system's regular operation. During its existence, the worm can release millions of microfilariae and live for approximately five to seven years. Infected individuals can infect others through mosquito bites if they have microfilariae in their blood[4]. Clinical signs never appear in the majority of affected individuals. Lymphoedema, a severe swelling of the limbs, and advanced form elephantiasis are symptoms of a lymphatic system that has worsened due to a long-term infection. The accumulation of fluid and swelling known as lymphedema is the consequence of the lymph system not working properly. Legs, arms, breasts, and genitalia are all impacted by this[5]. In most cases, these clinical indicators manifest many years following infection. Patients with disabilities face not just physical impairments but also social, emotional, and financial losses that worsen poverty and stigma[6].

In tropical Asia, Africa, and the Indian subcontinent, as well as certain parts of Latin America, it poses a serious threat to public health. Preventive chemotherapy is necessary to stop the spread of illness; in 2021, 882.5 million people in 44 nations were reportedly living in such locations7. Global baseline cases of lymphatic filariasis were estimated to be about 15 million people with lymphoedema and 25 million males with hydrocele. These symptoms of a chronic illness are still experienced by at least 36 million people. Preventing need-

less suffering and reducing poverty rates are both possible outcomes of eradicating lymphatic filariasis[8]. In an effort to reduce the burden of lymphatic filariasis and to halt the spread of the disease in affected communities, the World Health Organization has advocated for the mass drug administration (MDA) of DEC (Diethylcarbamazine) (6 mg/kg) and other anthelminthic medication combinations to all eligible individuals in affected areas once or twice a year. Although DEC has been used as an anti-filarial for 60 years, there is still no clear understanding of how it works[9]. Its impact on adult worms is very limited, and if therapy is interrupted, microfilariae can repopulate. Given these obstacles and the large number of people who are still affected, new treatments are necessary. Clinical outcomes for infected patients can be improved and noncompliance difficulties can be addressed by identifying the safe and effective therapeutic target for Brugia malayi, Wuchereria bancrofti, and Brugia timori [3,10]. Traditional treatments for lymphatic filariasis have made use of a number of plant chemicals. Azadirachta indica A. Juss, or neem tree (family Meliaceae), is primarily found in tropical areas, particularly in India and West Africa. Azadirachtin, a significant tetranortriterpenoid phytocompound found in Azadirachta indica and it is used as a complementary medicine in many diseases as antimicrobial, antimicrobial and antifilarial potential against the filarial parasite. Research on animal models has shown that the bioactive components of Azadirachta indica can inhibit inflammation, fight cancer, eliminate fungal infections, and speed up the healing process of wounds[11]. Moreover, both invivo and invitro studies on azadirachtin reports that it is nontoxic in toxic analysis. Therefore, in this study, based on the pharmacological effectiveness, azadirachtin is used as a possible therapeutic agent against filariasis. In 1977, Edward Munn proposed the idea that proteins in the intestines can function as "hidden antigens" that the immune system does not encounter during a natural infection and so does not trigger an allergic response in endemic populations. The importance of UDP-glucuronosyltransferases (GT) protein in macrofilaricidal activity was studied using small interfering RNA (siRNA) knockdown expression and thus reveals the importance of GT protein in worm survival. Based on this, the purpose of this study is to use insilico experiments to determine if azadirachtin is a viable treatment for lymphatic filariasis by evaluating its action against the intestinal UDP-glucuronosyltransferases proteins of Brugia malayi, Wuchereria bancrofti, and Brugia timori[12].

Materials and Methods

Sequence retrieval and Template Identification

The FASTA sequences of the intestinal target protein UDP-glucuronosyltransferases of A0A0K0J9I9, 319 amino acids (Brugia malayi), A0A1I8EHV2, 431 amino acids (Wuchereria bancrofti) and A0A0R3QRC9, 540 amino acids (Brugia timori), were retrieved from the Universal Protein Resource (UniProt) (Brugia timori). We used the Basic Local Alignment Search Tool (BLAST) search with default parameters to gather sufficient identical templates to create the 3D structures of intestinal proteins because, unfortunately, there is no data on their crystal structures[13,14].

Construction of 3D model using I-Tasser

Homology modeling was performed to resolve the 3-dimensional structure of UDP-glucuronosyltransferase protein of Brugia malayi, Wuchereria bancrofti and Brugia timori using I-TASSER (https://zhanglab.ccmb.med.umich.edu/I-TASSER/). An online program called the I-Tasser server can automatically anticipate the structural and functional annotation of a target macromolecule[15]. The PBD library is queried for the template protein, and the Monte Carlo simulation approach is used to assemble the fragments into a complete framework[16,17]. In order to build the misaligned parts, especially the loops and tails, ab initio modeling was also employed. The simulation technique is improved by spatial limitations, so the clustering decoys with the lowest energy model are picked. Eventually, the optimization of hydrogen bonds allows for identifying the best model based on the C score (Confidence score) function scores. A higher C-score value between − 5 and 2 indicates a higher confidence level in the constructed model[18].

Model refinement

Get the experimental structure right as a last step in predicting the protein's structure. The GalaxyRefine web server relaxed and subjected structures to stringent perturbations using dynamic simulations. The top most model obtained from the I-TASSER server was chosen and submitted to the GalaxyRefine server (http://galaxy.seoklab.org/). Rotamers were used to reestablish the side chain configurations, and their energy functions are determined by the CHARMM22 force field. The optimal structure was chosen after careful evaluation of all the possibilities provided by GalaxyRefine[19].

Structure validation of modeled protein

The online tool SAVES server validated the energy-minimized and refined 3D structure(https://saves.mbi.ucla.edu/).

The presence of the backbone of the protein was examined by evaluating the psi/phi Ramachandran plot obtained with PROCHECK[20]. ERRAT (http://services.mbi.ucla.edu/ERRAT/) is a well-known overall quality factor that evaluates the 3D construct constructed by counting the non-bonded atomic interactions and evaluating the error values through a notable crystal structure. Depending on the variation in consensus results, the topmost 3D structures were preferred for docking studies. Pymol version 2.0 is used to visualize these protein structures[21].

Prediction of Ligand Binding Sites

The UDP-glucuronosyltransferase proteins of Brugia malayi, Wuchereria bancrofti, and Brugia timori were analyzed using the Computed Atlas of Structure Surface Topography of proteins (CASTp) to identify possible ligand binding sites[22]. Using PyMOL, the outcomes were analyzed. Choosing the most likely binding cavities involved taking the area and volume of the anticipated sites into account[23].

Molecular docking simulation

The compounds azadirachtin (PubChem CID- 5281303) and diethylcarbamazine (PubChem CID-3052) were docked with the three-dimensional structure of the glucuronosyltransferase protein from Brugia malayi, Wuchereria bancrofti, and Brugia timori using the AutoDock tool (v4.2.6). Adding hydrogen atoms, merging less polar hydrogen molecules, dispersing Kollman charges, and storing the resulting 3D structures as PDBQT files were the steps used to construct these proteins[24]. Diethylcarbamazine and azadirachtin's three-dimensional structures were derived from the PubChem database. Incorporating Gasteiger's charges, polar hydrogens, non-polar hydrogen molecules, rotatable bonds, and storing in PDBQT format were the steps used to build the ligand structures. The Molecular Graphics Laboratory (MGL) Tools were utilized to import the produced target proteins and ligand. The assumption of rigidity in the target protein and flexibility in the ligand molecule has also been used in docking research. The following step, using the anticipated active site, is to produce the receptor's grid generation. Lastly, the docking parameter file was generated by running the auto dock application[25]. The potentials for hydrogen bonding, electrostatic interactions, desolvation, binding energy, and van der Waals contact between the ligand and protein will be examined. Pymol was used to visualize the interactions between the protein-ligand complexes[26].

ADME and toxicity prediction

Examining the molecular mechanisms

of drug distribution and individual response, as well as their therapeutic efficacy, requires an understanding of these ADME features27,28. Physicochemical characteristics, lipophilicity, water solubility, and pharmacokinetics were among the many parameters examined by the SwissADME web server29. In order to get the results, the ligand's smile format is uploaded to the SwissADME (http://www.swissadme.ch/)30.

Results and Discussion

Homology modeling

The 3-dimensional structure of glucuronosyltransferase proteins of Brugia malayi, Wuchereria bancrofti, and Brugia timori was constructed using I-Tasser. I-Tasser evaluates 3D structures through parameters such as C-score, TM-score, or RMSD score. Normally, C-score occurs between −5 to 2, whereas the C-score of a higher value implies that a specific predicted structure has high confidence. Template modeling score (TM-score) is a known specification for measuring structural similarity between two structures, whereas the native structure is known. GT_BM referred as glucuronosyltransferases protein of Brugia malayi, GT_WB for Wuchereria bancrofti, and GT_BT for Brugia timori. For the GT_BM protein, the top 10 threading templates used by I-TASSER are (1P1D,-8T2I, 7XS0, 7W6X, 6Z05, 8DEO, 4WYT, 7X7A, 3R0H, 2XKXA) and the C-score was found to be -3.42, the estimated TM-score was 0.34±0.11 and estimated RMSD was 14.7±3.6Å. For GT_WB, the top 10 threading templates used by I-TASSER are (6J31, 7LVY, 8GKN, 7W09, 7W09,7LVY-A,7W09, 6INFA, 6PNTA,7LVYA) and the C-score was found to be -0.99, estimated TM-score was 0.59±0.14 and the estimated RMSD was 9.2±4.6Å. Finally for the GT_BT, the top 10 threading templates used by I-TASSER are (5GL5, 7LVY, 8GKN, 7W09, 5GL5, 7LVY, 5GL5, 6INF, 6PNT, 7LVY) and C-score was found to be -2.39, the estimated TM-score was 0.43±0.14 and the estimated RMSD was 13.3±4.1Å. The normalized Z-score corresponding to the threading templates for GT_BM, GT_WB and GT_BT was found to be 3.91, 3.48, 1.82, respectively. The normalized Z-score > 1 implies that the generated 3D model is aligned well. Using the GalaxyRefine server, the best models were refined using CASP method and the final refined models mentioned in Figure 1 (a-c) were used for further docking studies.

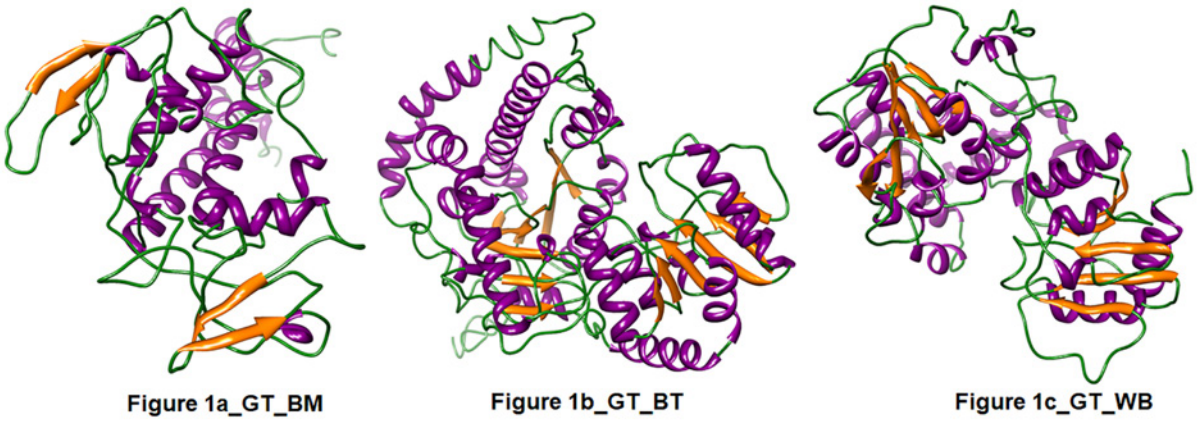


Figure 1a_GT_BM Figure 1b_GT_BT Figure 1c_GT_WB

Figure 1(a-c): The Three-Dimensional structure of the UDP-glucuronosyltransferases (GT) of a(Brugia malayi (BM), b) Brugia timori (BT) and c) Wuchereria bancrofti (WB).

Protein validation

The ERRAT and PROCHECK programs were used via the SAVES server to validate the three-dimensional structures of the GT BM, GT WB, and GT BT proteins. For atomic interactions that are not bound, ERRAT displays the total quality factor. The commonly acknowledged range for a high-quality model is larger than 50, and higher scores suggest higher quality. In GT_BM, the ERRAT score was found to be 98.81, 97.36 for the GT_BM protein and 98.5 for GT_BT model, which is an acceptable score for a typical 3Dmodels. PROCHECK determines the geometrical roles of the residues in the developed glucuronosyltransferase proteins in order to assess their stereochemical characteristics. The PROCHECK results show that the distribution of residues in a different environment is acquired by the Ramachandran plot of the modeled protein molecules.

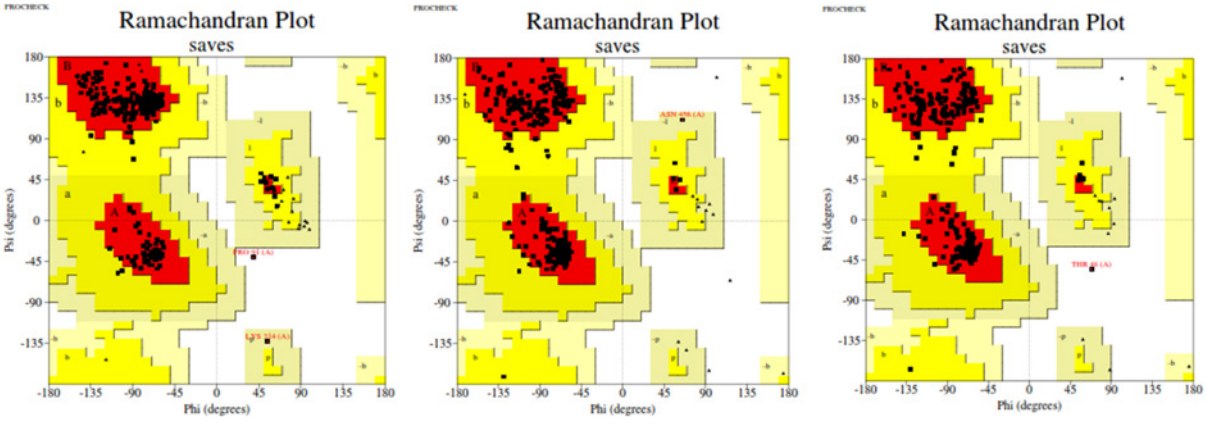


Figure 2 : Ramachandran plot values for the protein a) GT_BM, b)GT-WB, c)GT-BT

In GT_BM protein, among 319 residues, 271 residues (95.1%) were spotted in the most favored region, 13 residues (4.6%) were observed in the additional allowed region, 1 residue (0.4%) was placed in the generously allowed region, and no residues in the disallowed region. In GT_WB, among 540 residues, 483 res-

idues (97.2%) were spotted in the most favored region, 13 residues (2.6%) were observed in the additional allowed region, 1 residue (0.2%) was placed in the generously allowed region, and no residues in the disallowed region. Similarly, for GT_BT among 431 residues, 381 residues (96.9%) were spotted in the most favored region, 11 residues (2.8%) were observed in the additional allowed region, no residue was placed in the generously allowed region, and 1 residue (0.3%) in the disallowed region (Figure 2a-c). Accordingly, the outcome of PROCHECK implies the quality of the selected 3-dimensional protein structure.

Active site Prediction

CASTp gives precise measurements of the predicted binding site's surface area and volume of the pocket that makes up the site. After utilizing PyMOL to view each binding pocket, the optimal pockets were selected based on their size and volume, which were comparatively large. Binding sites that were predicted to have tiny volumes and areas without any apertures were disregarded. The Volume (SA)/Å3 for GT_BM, GT_WB and GT_BT was 941.641, 959.439, and 959.439, respectively. The area (SA)/Å2 for GT_BM, GT_WB and GT_BT was found to be 1381.373, 1431.502 and 3556.478, respectively.

Swiss ADME

Both the plant-derived chemical Azadirachtin and the commercially available medicine Diethylcarbamazine for lymphatic filariasis were subjected to SwissADME analysis to ascertain their physicochemical, lipophilicity, water solubility, pharmacokinetics, druglikeness, and medicinal chemistry properties. Approximately half of the natural compounds with which we worked on pharmacokinetic and drug-likeness prediction models exhibited promising results. Although natural products have their own unique set of physiochemical properties, the majority of chemicals generated from plants do not follow the guidelines laid out by Lipinski and others in the ADMET database.The detailed ADME results are depicted in Table 1.

Table 1: ADME prediction of azadirachtin in comparison with Diethylcarbamazine by SwissADME

Compounds	No of hydrogen bonds acceptor	No of hydrogen bond donars	TPSA (Å2)	Lipophilicity LogP (iLOGP)	Water Solubility LogS (ESOL)	Medicinal Chemistry Synthetic accessibility (1 to 10 range)
Azadirachtin	16	3	215.34	3.9	-4.34	8.11
Diethylcarbamazine	2	0	26.79	2.68	-0.99	2.3

Molecular docking analysis

Molecular docking and the affinity between a ligand and each glucuronosyltransferase protein receptor were performed using AutoDock vina. Following the preparation of protein and ligand, a grid map was generated to investigate the presence of additional elements that CASTp might not have identified. Different conformers for each ligand were searched for using the Lamarckian algorithm. We used binding energies in kcal/mol to represent all protein-ligand binding affinities. Docking data were displayed in Table 2 for the substances Azadirachtin and Diethylcarbamazine. The results showed the binding energies and amino acid interactions with selected intestinal UDP-glucuronosyltransferase proteins from Brugia malayi, Wuchereria bancrofti, and Brugia timori.

Table 2: Molecular docking results of intestinal glucuronosyltransferase protein complex with Azadirachtin and Diethylcarbamazine using Auto dock.

Compounds	Binding energies (Kcal/mol)	vdW + Hbond + desolv Energy (Kcal/mol)	Electrostatic Energy (Kcal/mol)	Total internal energy (Kcal/mol)	Inhibition Constant, Ki	Torsional energy (Kcal/mol)	Interacting residues
GT_BM _Azadirachtin	-12.78	-14.56	-0.30	+28.06	432.25 pM	+2.09	ASN 224, HIE 145, ASP 222
GT_BM _Diethylcarbamazine	-5.52	-6.14	+0.03	+0.03	90.65 uM	+0.60	HIE 145
GT_BT _ Azadirachtin	-14.81	-16.90	-0.10	+28.25	13.87 pM	+2.09	No hydrogen bond was found
GT_BT _ Diethylcarbamazine	-4.99	-5.55	-0.04	+23.60	220.55 uM	+0.60	HIE 36
GT_WB _ Azadirachtin	-12.92	-14.66	-0.05	+28.16	340.80 pM	+1.79	GLH 142, SER 372, GLN 392, VAL 300
GT_WB _ Diethylcarbamazine	-6.07	-6.63	+23.59	+23.59	35.78 uM	+0.60	GLH 142

Figure 3 (a-f). Highest docked score of -14.81 kcal/mol was showed by azadirachtin aginst glucuronosyltransferase protein of Brugia timori and lowest docked score of -4.99 kcal/mol against diethylcarbamazine. The docked poses were visualized in pymol to check the significant amino acids interaction with ligand. Asparagine 224, Histidine 145, Aspartic Acid 222, Glutamic acid 142, Serine 372, Glutamine 392, VAL 300 residues were found to be actively interacting with the ligand aza-

dirachtin. Overall, in comparison with Diethylcarbamazine, Azadirachtin had the highest binding affinity of -12.78 kcal/mol, -14.81 kcal/mol and -12.92 kcal/mol for GT_BM, GT_WB and GT_BT, respectively.

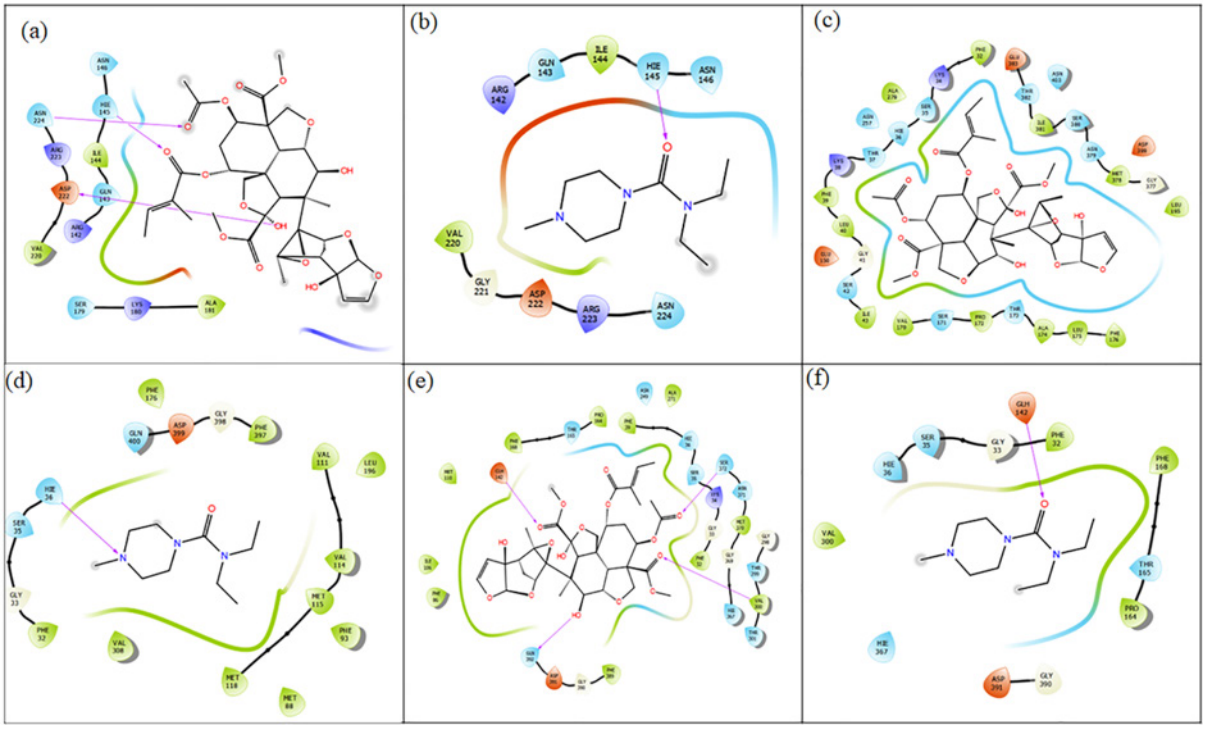


Figure 3(a-f): Molecular docking illustrations showing ligand-proteins interactions of (a) GT_BM _Azadirachtin, (b) GT_BM _Diethylcarbamazin, (c) GT_BT _ Azadirachtin, (d) GT_BT_ Diethylcarbamazine, (e) GT_WB_Azadirachtin, (f) GT_WB _ Diethylcarbamazine

Conclusion

Lymphatic filariasis, caused by the parasites Brugia malayi, Wuchereria bancrofti, and Brugia timori, affects an estimated 70 million people globally. Global eradication attempts were hindered by the limited availability of effective treatments to kill adult filarial parasites. Research has demonstrated that antibodies and medications can successfully attack parasites in their digestive systems. Results from invitro experiments show that this protein is critical for adult worms to stay alive. Alexander F. Flynn et al identified that gene-expression knockdown of intestinal glucuronosyltransferases protein shows rapid decrease in motility, fecundity, and microfilarial release. The possibility of the intestinal UDP-glucuronosyltransferase of Brugia malayi, Wuchereria bancrofti, and Brugia timori as a therapeutic target protein for filarial infection and illness control was explored in this study. It was necessary to create a suitably validated protein structure since the structures of BM, GT, and BT glucuronosyltransferases had not been identified experimentally. Hot tropical re-

gions, like those of India and West Africa, are typical habitats for neem trees. The bitter taste of this tree's leaves and bark is caused by azadirachtin, a triterpenoid biochemical component. Research indicates that this tree's medicinal capabilities extend to treating a wide range of diseases, including infections caused by bacteria, inflammation, cancer, malaria, ulcers, and, most notably, filariasis. Azadirachtin was found to have a similarly deadly effect on microfilariae of different species, according to multiple invitro experiments. Here, we investigated how azadirachtin interacted with the Brugia malayi, Wuchereria bancrofti, and Brugia timori UDP-glucuronosyltransferases (UGTs) protein in the intestines. To assess the inhibitory property of the plant-derived Azadirachtin and to compare it to that of Diethylcarbamazine, a drug that is currently on the market for the treatment of filariasis, researchers used molecular informatics methods such as molecular docking, physicochemical profiling, and pharmacological profiling. Azadirachtin has a potent inhibitory impact on the glucuronosyltransferases (UGTs) of three different filarial parasites, including Brugia malayi, Wuchereria bancrofti, and Brugia timori, according to molecular docking studies. This suggests that it may kill adult filarial parasites.

Conflict of Interest

None

Funding

None

Reference

1. Shirley H, Orriols A, Hogan D, et al. Lymphatic filariasis in Zambia: A scoping review protocol. PLoS One 2023;18(10):e0292237, doi:10.1371/journal.pone.0292237
2. Djuardi Y, Jannah IF, Supali T. IgG4 antibodies against Bm14 as an evaluation tool of mass drug administration in a co-endemic area of Brugia timori and Wuchereria bancrofti. Acta Trop 2022;227(106278, doi:10.1016/j.actatropica.2021.106278
3. Simonsen PE, Mwakitalu ME. Urban lymphatic filariasis. Parasitol Res 2013;112(1):35-44, doi:10.1007/s00436-012-3226-x
4. Chakraborty S, Gurusamy M, Zawieja DC, et al. Lymphatic filariasis: perspectives on lymphatic remodeling and contractile dysfunction in filarial disease pathogenesis. Microcirculation 2013;20(5):349-64, doi:10.1111/micc.12031
5. Farrow W. Phlebolymphedema-a common underdiagnosed and undertreated

problem in the wound care clinic. J Am Col Certif Wound Spec 2010;2(1):14-23, doi:10.1016/j.jcws.2010.04.004

6. Bunke N, Brown K, Bergan J. Phlebolymphemeda: usually unrecognized, often poorly treated. Perspect Vasc Surg Endovasc Ther 2009;21(2):65-8, doi:10.1177/1531003509337155
7. Pinto JA, Pinillos L, Villarreal-Garza C, et al. Barriers in Latin America for the management of locally advanced breast cancer. Ecancermedicalscience 2019;13(897, doi:10.3332/ecancer.2019.897
8. Fimbo AM, Minzi OMS, Mmbando BP, et al. Prevalence and Correlates of Lymphatic Filariasis Infection and Its Morbidity Following Mass Ivermectin and Albendazole Administration in Mkinga District, North-Eastern Tanzania. J Clin Med 2020;9(5), doi:10.3390/jcm9051550
9. Ramaiah KD, Vanamail P, Yuvaraj J, et al. Effect of annual mass administration of diethylcarbamazine and albendazole on bancroftian filariasis in five villages in south India. Trans R Soc Trop Med Hyg 2011;105(8):431-7, doi:10.1016/j.trstmh.2011.04.006
10. Vasuki V, Hoti SL, Subramanian S, et al. Multi-centric evaluation of a stage-specific reverse transcriptase-polymerase chain reaction assay as a xenomonitoring tool for the detection of infective (L(3)) stage Wuchereria bancrofti in vectors. Indian J Med Res 2021;154(1):132-140, doi:10.4103/ijmr.IJMR_713_19
11. Specht S, Suma TK, Pedrique B, et al. Elimination of lymphatic filariasis in South East Asia. BMJ 2019;364(k5198, doi:10.1136/bmj.k5198
12. Chesnais CB, Awaca-Uvon NP, Vlaminck J, et al. Risk factors for lymphatic filariasis in two villages of the Democratic Republic of the Congo. Parasit Vectors 2019;12(1):162, doi:10.1186/s13071-019-3428-5
13. Kari S, Murugesan A, Thiyagarajan R, et al. Bias-force guided simulations combined with experimental validations towards GPR17 modulators identification. Biomed Pharmacother 2023;160(114320, doi:10.1016/j.biopha.2023.114320
14. Anjugam M, Iswarya A, Sibiya A, et al. Molecular interaction analysis of beta-1, 3 glucan binding protein with Bacillus licheniformis and evaluation of its immunostimulant property in Oreochromis mossambicus. Fish Shellfish Immunol 2022;121(183-196, doi:10.1016/j.fsi.2021.12.044

15. Kaliamurthi S, Selvaraj G, Selvaraj C, et al. Structure-Based Virtual Screening Reveals Ibrutinib and Zanubrutinib as Potential Repurposed Drugs against COVID-19. Int J Mol Sci 2021;22(13), doi:10.3390/ijms22137071

16. Selvaraj C, Dinesh DC, Krafcikova P, et al. Structural Understanding of SARS-CoV-2 Drug Targets, Active Site Contour Map Analysis and COVID-19 Therapeutics. Curr Mol Pharmacol 2022;15(2):418-433, doi:10.2174/1874467214666210906125959

17. Selvaraj C, Selvaraj G, Mohamed Ismail R, et al. Interrogation of Bacillus anthracis SrtA active site loop forming open/close lid conformations through extensive MD simulations for understanding binding selectivity of SrtA inhibitors. Saudi J Biol Sci 2021;28(7):3650-3659, doi:10.1016/j.sjbs.2021.05.009

18. Smak P, Chandrabose S, Tvaroska I, et al. Pan-selectin inhibitors as potential therapeutics for COVID-19 treatment: in silico screening study. Glycobiology 2021;31(8):975-987, doi:10.1093/glycob/cwab021

19. Choudhary P, Bhowmik A, Chakdar H, et al. Understanding the biological role of PqqB in Pseudomonas stutzeri using molecular dynamics simulation approach. J Biomol Struct Dyn 2022;40(9):4237-4249, doi:10.1080/07391102.2020.1854860

20. Selvaraj C, Dinesh DC, Panwar U, et al. Structure-based virtual screening and molecular dynamics simulation of SARS-CoV-2 Guanine-N7 methyltransferase (nsp14) for identifying antiviral inhibitors against COVID-19. J Biomol Struct Dyn 2021;39(13):4582-4593, doi:10.1080/07391102.2020.1778535

21. Chinnasamy S, Selvaraj G, Selvaraj C, et al. Combining in silico and in vitro approaches to identification of potent inhibitor against phospholipase A2 (PLA2). Int J Biol Macromol 2020;144(53-66, doi:10.1016/j.ijbiomac.2019.12.091

22. Selvaraj C, Chandra I, Singh SK. Artificial intelligence and machine learning approaches for drug design: challenges and opportunities for the pharmaceutical industries. Mol Divers 2022;26(3):1893-1913, doi:10.1007/s11030-021-10326-z

23. Selvaraj C, Panwar U, Dinesh DC, et al. Microsecond MD Simulation and Multiple-Conformation Virtual Screening to Identify Potential Anti-COVID-19 Inhibitors Against SARS-CoV-2 Main Protease. Front Chem 2020;8(595273,

doi:10.3389/fchem.2020.595273

24. Chinnasamy S, Selvaraj G, Kaushik AC, et al. Molecular docking and molecular dynamics simulation studies to identify potent AURKA inhibitors: assessing the performance of density functional theory, MM-GBSA and mass action kinetics calculations. J Biomol Struct Dyn 2020;38(14):4325-4335, doi:10.1080/07391102.2019.1674695

25. Omer A, Suryanarayanan V, Selvaraj C, et al. Explicit Drug Re-positioning: Predicting Novel Drug-Target Interactions of the Shelved Molecules with QM/MM Based Approaches. Adv Protein Chem Struct Biol 2015;100(89-112, doi:10.1016/bs.apcsb.2015.07.001

26. Muralidharan AR, Selvaraj C, Singh SK, et al. Structure-Based Virtual Screening and Biological Evaluation of a Calpain Inhibitor for Prevention of Selenite-Induced Cataractogenesis in an in Vitro System. J Chem Inf Model 2015;55(8):1686-97, doi:10.1021/acs.jcim.5b00092

27. Jinying W, Keming L, Hanqing T, et al. Role and anti-inflammatory mechanisms of acupuncture and moxibustion therapy on pain relief through NOX-ROS-NLRP3 pathway in CCI rats models. Mol Biol Rep 2023;50(11):9367-9378, doi:10.1007/s11033-023-08858-8

28. Ezhilarasan D, Shree Harini K, Karthick M, et al. Ethyl gallate concurrent administration protects against acetaminophen-induced acute liver injury in mice: An in vivo and in silico approach. Chem Biol Drug Des 2023, doi:10.1111/cbdd.14369

29. Shiammala PN, Duraimutharasan NKB, Vaseeharan B, et al. Exploring the artificial intelligence and machine learning models in the context of drug design difficulties and future potential for the pharmaceutical sectors. Methods 2023;219(82-94, doi:10.1016/j.ymeth.2023.09.010

30. Mansouri K, Kleinstreuer N, Abdelaziz AM, et al. CoMPARA: Collaborative Modeling Project for Androgen Receptor Activity. Environ Health Perspect 2020;128(2):27002, doi:10.1289/EHP5580.